Proc. Indian Acad. Sci. (Earth Planet. Sci.), Vol. 93, No. 3, August 1984, pp. 283–308.

Rocket borne studies of electron density irregularities in equatorial D and E regions

S PRAKASH and R PANDEY

Physical Research Laboratory, Ahmedabad 380 009, India.

Abstract. Electron density irregularities in the equatorial D and E regions have been studied using ground-based and rocket-borne experiments. In this paper this subject is reviewed with an emphasis on the rocket-borne measurements of electron density and electric field structures and other parameters relevant for identifying processes responsible for generation of electron density irregularities. These studies have led to the identification of various causative mechanisms, in terms of plasma and neutral dynamical processes for producing irregularities. Based on these mechanisms, the irregularities are classified and discussed. There are many observations which have eluded explanation and hence call for sustained efforts.

Keywords. Rocket-borne studies; electron density irregularities; D and E regions; causative mechanisms.

1. Introduction

The upper atmospheric plasma is a unique plasma laboratory provided by nature, which is ideal for studying various plasma processes otherwise difficult to study in the laboratory. Three distinct plasma conditions are realised in different parts of upper atmosphere. In the E region only electrons are magnetised ($R_i > 1$, $R_e < 1$), in the F region both ions and electrons are magnetised ($R_i < 1$, $R_e < 1$) while in the D region both ions and electrons are unmagnetised ($R_e > 1$, $R_e > 1$). Here $R_{i,e}$ is the ratio of ion (electron) neutral collision frequency and ion (electron) gyrofrequency. The major events in the experimental study of electron density irregularities in the equatorial D and E regions are: (i) Establishment of an ionosonde in low geomagnetic latitudes (in Peru) during late thirties and study of the anomalous scattering region in the E region and its association with the equatorial electrojet. (ii) Establishment of a powerful VHF backscatter radar at Jicamarca (Peru) and study of the structure and dynamics of the 3 m irregularities in the E region during the early sixties. (iii) Establishment of a rocket launching station and VHF radar at Thumba, India (TERLS) and study of electron density irregularities in a wide range of scale sizes and associated parameters during the late sixties and early seventies. (iv) Study of irregularities in horizontal and vertical electric field associated with electron density irregularities during the late seventies and early eighties.

The irregularities in E region close to the dip equator were first detected as anomalous scattering regions with an ionosonde at Huancayo during 1937. These echoes, observed in E region during most of the daytime, were termed q-type of sporadic E (E_{sq}). Matsushita (1951) showed that the strength of the E_{sq} and equatorial electrojet are well correlated. VHF forward scatter radar studies over a transequatorial path showed that scattering was caused by electron density irregularities embedded in the electrojet plasma (Bowles *et al* 1960; Bowles and Cohen 1962) and occurred in the

altitude range of about 95–100 km. This agreed well with the electrojet current system (Singer *et al* 1951) and it was further inferred that these irregularities are field-aligned. This inference was confirmed by the observations of an obliquely looking radar at Huancayo, Peru (Egan 1960). Studies with the VHF backscatter radar at Jicamarca, Peru have significantly contributed to the field of equatorial electron density irregularities. The Jicamarca radar operates at about 50 MHz which corresponds to the irregularity scale size of about 3 m. These studies have given valuable information on various features of the irregularities like, the spatial distribution and drift velocity together with the region of occurrence, etc. On the basis of the Doppler spectral characteristics of the radar echoes which are mainly from the 3 m irregularities, the irregularities have been classified as types I and II (Bowles *et al* 1960, 1963; Bowles and Cohen 1962; Cohen and Bowles 1967; Balsley 1969). The type I Doppler spectra are characterised by a narrow spectral width corresponding to a Doppler shift from the transmitted frequency by about 120 ± 20 Hz. This Doppler shift corresponds to the drift velocity of the echoing region close to the ion acoustic velocity in the medium. Further, this Doppler shift was independent of the antenna elevation angle. Similar results were obtained at Thumba (Prakash *et al* 1974). Type I irregularities were observed only when the electrojet currents exceeded a critical value suggesting a threshold drift velocity requirement for their generation. Theories to explain various features of the type I irregularities have been proposed (Farley 1963; Bunneman 1963; Rogister 1971; Sato 1972; Weinstock and Sleeper 1972; Kaw 1972; Lee *et al* 1974; Keskinen 1981).

The Doppler spectra for type II irregularities were broader than for type I. From the shift of the Doppler spectra with the elevation angle, it has been found that these irregularities generally drift horizontally (Balsley 1967). When the electrojet currents are weak and also when the antenna is pointed vertically upward, type II irregularities dominate over type I. Type II irregularities have been extensively studied using the range time intensity (RTI) diagrams obtained at the Jicamarca facility. The region of occurrence of type II irregularities changes drastically during different times of the day. During daytime they are observed in one altitude region whereas during evening and night they are observed in many different altitude regions (Fejer *et al* 1975).

The ground-based VHF backscatter radars at Jicamarca, Thumba and Addisababa have proved to be a very powerful tool to study some of the bulk properties of the ionization irregularities. However, being a ground-based technique, it does not have sufficient spatial resolution for studying many of the plasma processes taking place in this region. In addition the radar does not give many of the relevant localised parameters of the medium which have important bearing on the understanding of plasma processes. As the radar responds only to 3 m irregularities the range of wavelengths at which a particular process is operative cannot be ascertained. This makes *in situ* measurements essential. Indeed, *in situ* and ground-based measurements complement each other; ground-based techniques give bulk properties of the medium while *in situ* measurements give measurements with high resolution. There are still many intriguing and unresolved features of the electrojet irregularities and hence require sustained efforts, both through *in situ* and ground-based experiments supported by theoretical studies.

The parameters relevant for the production of electron density irregularities are the horizontal and vertical electric field and the structures therein, relative streaming velocity of ions and electrons, gradients in the plasma density, neutral winds and the collision frequency parameters R_i and R_e. The study of DC electric field even with

most sophisticated techniques (Sartiel 1977) has not been fruitful. Its direction can however be determined with ground-based/rocket-borne magnetometers and VHF radar. Through various indirect measurements, the east-west (horizontal) electric field has been estimated to be about 0·5 to 1 mV/m when the electrojet currents are at its maximum. The corresponding vertical Hall polarization electric field around the peak of the electrojet ($\approx$ 106 km) is estimated to be $\approx$ 10 to 15 mV/m. During daytime normal electrojet, the horizontal electric field is eastward while the vertical field is upwards. During most of the nights and during daytime counter electrojet periods, the horizontal and the vertical electric fields are reversed in direction.

The relative streaming velocity of ions and electrons is derived from the currents as determined with rocket-borne magnetometers and the absolute electron density as determined with a mutual admittance probe. While the gradients in the plasma density along the rocket trajectory can be easily measured, determination of the horizontal gradients is difficult. Although large scale neutral winds can be measured with the vapour release technique, it is difficult to measure localised winds. In addition, the plasma measurements and the vapour release experiments cannot be carried out simultaneously. It has not been possible to determine R_i and R_e experimentally and one has to take recourse to model calculations. The discrepancy of 3 km in the peak altitude of the electrojet observed experimentally and that estimated through model calculation (Subbaraya *et al* 1972) indicate that the R_i and R_e values from the model calculations should be increased by a factor of three to account for the observed discrepancy. As no direct measurement of collision frequencies is available and as they are derived indirectly, large errors in them are quite possible.

A comprehensive study of ionization irregularities in the *D* and *E* region was carried out from Thumba (dip 0°·47′S) using rocket-borne Langmuir probes to measure electron density and irregularities therein (Prakash and Subbaraya 1967), resonance (mutual admittance) probe for absolute electron density measurement (Prakash *et al* 1971; Rao and Prakash 1978), proton precession magnetometer of Dr T S G Sastry for electric currents measurement (Sampath 1976), and double probes for the measurement of horizontal and vertical electric field and irregularities therein (Pandey 1981; Pal *et al* 1983). Rocket-borne experiments have also been carried out recently in the American zone using Langmuir probes (Klaus and Smith 1978) and double probes to measure horizontal electric field (Pfaff *et al* 1982). Experiments employing different payload combinations have been conducted from Thumba to measure simultaneously various ambient parameters of the medium. Some of the combinations of the probes employed are shown in figures 1 and 2 together with the arrangements of various sensors.

These studies have given a host of new information on the shape, size, region of occurrence and spectrum of electron density irregularities, and their relationship with other ambient parameters like electron density and gradients, electric fields and electron streaming velocity relative to ions, etc. For convenience, irregularities have been classified according to their generation mechanism and scale size range in which they are observed. In this classification (Prakash *et al* 1973), the irregularities with scale sizes larger than 300 m have been termed type L; with scale sizes in the range 30–300 m as type M, and with scale sizes in the range 1–15 m as type S. The 30–300 m range has now been extended to 15–300 m range. The results in this new range of wavelength are similar to those in the 30–300 m range. Detailed classification of the irregularities is as follows: (i) large scale irregularities (type L) observed in *E*-region. (ii) due to cross field instability mechanism (type M_c and S_c) observed in the *E*-region where the ambient

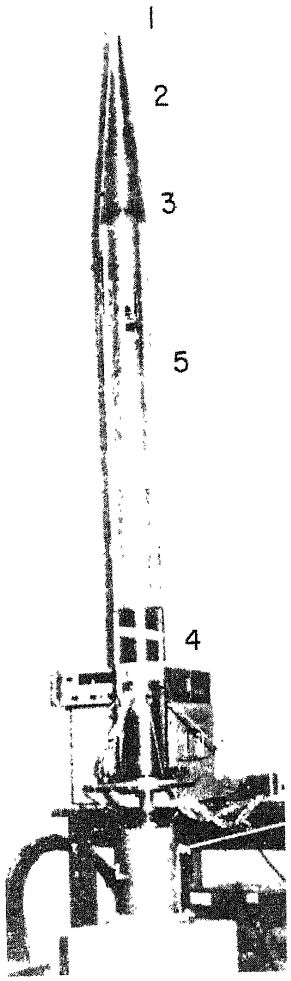

Figure 1. An integrated multiprobe payload of Langmuir probe, resonance probe, propagation experiment and UV detectors. The sensor **1** at the top of the rocket is for Langmuir probe, the conical body **2** and the cylindrical body **4** are respectively the receiver and exciter for the resonance probe. The fibreglass section **3** houses the propagation experiment and the cutout **5** is for the UV payload. The nose cone is mounted on the shake table.

electric fields are in the same direction as the gradients in the electron density. (iii) due to streaming of electrons (type S_s) observed near the peak of the electrojet. (iv) due to neutral turbulence (type M_n and S_n) observed in the D region. (v) rocket-induced observed near the apogee of the rocket. The rocket induced irregularities will not be discussed here.

Before discussing the electron density irregularities we elaborate on the salient features of the electron density profile during different times of the day, *viz* day, evening and night. Representative profiles for these periods, although not corresponding to the same day, are shown in figure 3. It is seen that during daytime the electron density increases rapidly from 60 to 110 km altitude and thereafter it becomes almost constant

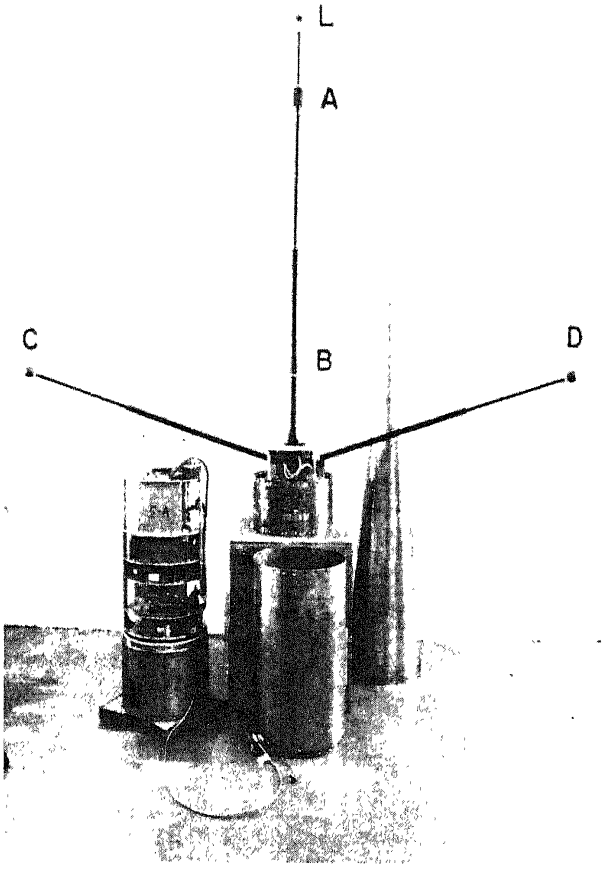

Figure 2. Mountings of the Langmuir probe and double probe sensors to measure the electron density and electric fields. The sensor L on the top of the central boom is the Langmuir probe sensor. The two cylindrical sensors A and B are to measure vertical electric field. The sensors at the ends of the two sideways deployable booms are to measure horizontal electric field. A part of the nose cone section along with the integrated payload decks is also shown.

attaining a value of about 1·5 to 2×10^5 electrons per cc. On some days a decrease of 10% in electron density is observed in the 115 km region. During daytime the altitude region from 82 to 93 km is characterised by a sharp gradient in electron density. Around sunset the *E* region density decreases rapidly through recombination processes. The density profile does not remain smooth and both upward and downward gradients are present. During evening the steepest gradients are observed around 85 km. The nighttime profile in figure 3 is much more irregular than the daytime and the evening time profile wherein a larger number of upward and downward gradient regions are observed. Another important feature is a well-developed valley around 130 km which is quite a common feature during night.

We discuss in this paper the electron density irregularities during different times of the day and under varied ionospheric conditions.

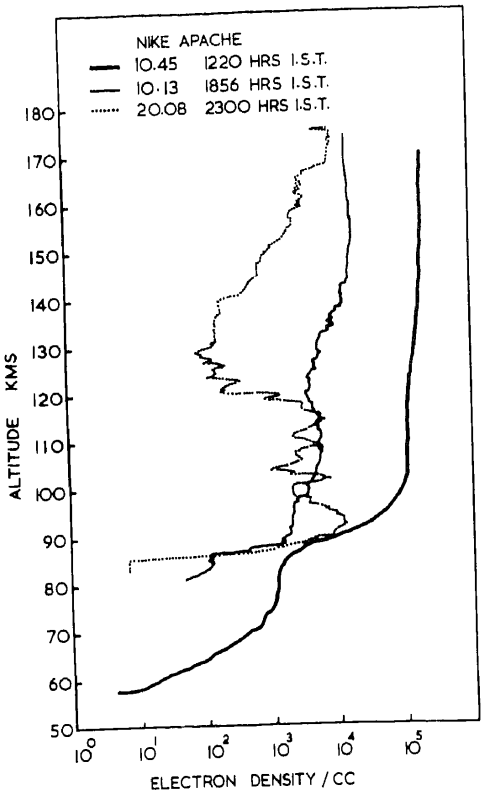

Figure 3. Typical electron density profiles obtained during the daytime, evening time and nighttime respectively, from the flights 10·45, 10·13 and 20·08 conducted from Thumba.

2. Large scale irregularities (type L)

The most illustrative example of the large scale irregularities is shown in figure 4 (Prakash *et al* 1972) which is a nighttime electron density profile obtained during the flight No. 20·08 on 29 August 1968 at 2300 hr (IST) from Thumba. The thin line and thick line correspond to the density profile during rocket ascent and descent respectively. The two profiles show general agreement as seen in figure 4. Both the profiles have a large number of structures in the altitude range 90 to 120 km having scale size of the order of a few km. In the most prominent structures the density varied by a factor as large as 25 thereby giving them the appearance of layers. Since there is a good matching of the altitudes, where the structures during ascent and descent are observed, it suggests that these structures have a large horizontal extent (scale size). For example around 100 km altitude where the most prominent structure is observed, the horizontal range of the rocket is about 60 km. Hence this structure should have a horizontal (east-west) extent of at least 60 km. The structures observed on other flights from Thumba (Sinha 1976) and from Chilka (Klaus and Smith 1978) during night were smaller in amplitude and the correlation between ascent and descent was therefore not as good as for the flight 20·08. Figure 5 gives the electron density profile over SHAR at 2103 hrs IST. It can be seen that some of the structures in the *E* region during ascent and

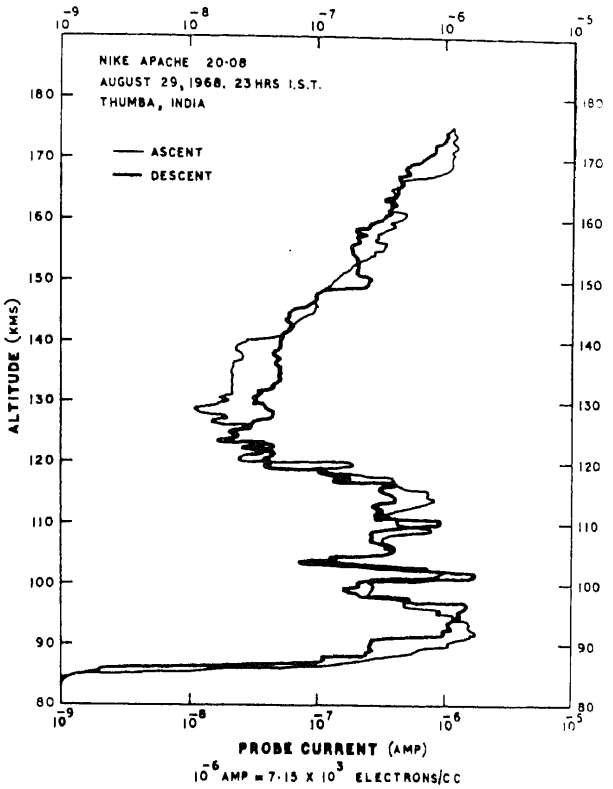

Figure 4. Profile of the electron current obtained during the 20·08 nighttime flight from Thumba. The density profile can be constructed from this profile using the given conversion factor. The large scale irregularities (type L) giving the appearance of layers of ionization are clearly seen both during rocket ascent and descent.

descent are similar indicating that the horizontal scale size of the structures is of the order of few hundred km. For this flight the ascent and descent are horizontally separated by more than 400 km. Therefore the large scale irregularities have a vertical scale size of a few km with associated horizontal scale size of hundreds of km in the east-west direction.

During daytime, type L irregularities have been observed only on two rocket flights carried out during the partial and full counter electrojet events (Prakash *et al* 1979a). One of the rocket flights C05-16 on 17 August 1972 at 1532 hrs IST was during a counter electrojet and the other C-22 on 21 April 1975 at 1341 hrs IST was during a partial counter electrojet period as defined by Rastogi (1974). The C05-16 flight was on a magnetically quiet day ($A_p = 6$) while the C-22 was on a magnetically disturbed day ($A_p = 23$). Figure 6 shows the electron density profiles obtained from these flights. During the C-22 flight the ionization layer was observed around 91 km, and during the C05-16 flight around 95 km as single layers. During both these flights the ionograms showed blanketing type of sporadic-E (E_{sb}). It may be pointed out that the ionization layers under normal daytime electrojet conditions were never observed.

The generation mechanism of type L irregularities is not yet clear. As pointed out earlier, type L irregularities appear as single layers during daytime while during

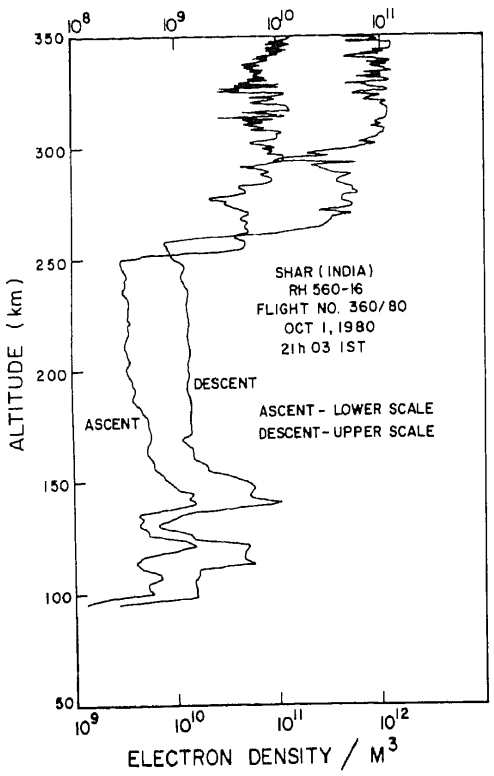

Figure 5. Electron density *vs* altitude profile obtained on 1 October 1980 during strong spread-*F*. The density scales for the descent is shifted towards right by a factor of ten. The lower scale gives the electron density M^{-3} for ascent and the upper scale gives the electron density for descent.

nighttime they appear as multilayers indicating that their mechanism of generation is somewhat different. Blanketing type of layers have been observed at mid-latitudes (*e.g.* Smith and Mechtly 1972) and have been explained invoking the wind shear theory (Whitehead 1961; Axford 1963). Axford (1963) demonstrated the theory to be inapplicable at the equator where the geomagnetic field lines are horizontal. It was shown that for this field line geometry, the polarization fields generated due to the dynamo action of a height varying east-west neutral wind are not electrically loaded and hence are fully developed, making the electric field $[E + (W \times B)]$ in the frame of reference of the wind to be zero. Therefore, according to the above theory, the wind shears in the neutral winds at the equator will not be effective in the formation of ionization layer.

Kato (1973) showed that due to the finite curvature of the geomagnetic field lines, the polarization fields due to height varying eastward winds are not developed fully and hence the nighttime ionization layers at the equator can be explained using these winds. From his theory the ion convergence rate at the equator was much smaller than at the mid-latitudes. Using two-dimensional gravity wave winds and taking the curvature of geomagnetic field lines into account Anandrao *et al* (1977) showed that Kato's results are an overestimate. Prakash and Pandey (1979) showed that for three-dimensional

gravity wave winds, the wavenumber along B plays a very important role in determining the extent of shorting of the gravity wave-induced polarization fields. For the gravity wave winds, the polarization fields are heavily loaded except when $k_x = 0$ where k_x is the wavenumber along B. Unlike the model proposed by Kato (1973) the one proposed by Prakash and Pandey (1979) does not require bending of the geomagnetic field lines for the shorting of the wind-induced polarization fields. The ion convergence rate at the equator below 120 km altitude as calculated using the three-dimensional model is larger than that in the mid-latitudes. The shears in the gravity wave winds can therefore account for the production of type L irregularities at least during nighttime (Prakash and Pandey 1979).

3. Irregularities produced through crossfield plasma instability

Laboratory plasma experiments (Simon 1963; Hoh 1963) under crossed electric and magnetic field configuration, and in the presence of non-uniform plasma density showed that the plasma becomes unstable when either the electric field or the magnetic field reached a critical value. Subsequent applications of Simon's theory to ionospheric E region plasma (Maeda *et al* 1963; Knox 1964; Morse 1965; Reid 1968) were followed by the theory of Rogister and D'Angelo (1970) and Sudan *et al* (1973), which demonstrated the E region plasma to be unstable at long wavelength perturbations in the medium when the large scale electric field and the electron density gradients were in the same direction. Electron density irregularities in the scale size range 30–300 m were observed on all flights (except one which was during very weak electrojet condition) from Thumba (Prakash *et al* 1970, 1971, 1972a) in regions where the above conditions are satisfied. These have been designated here as type M_c. In the subsequent sections we discuss the salient features of the type M_c and S_c irregularities.

3.1 *Medium scale irregularities (type M_c)*

3.1a *Region of occurrence*: As shown earlier in figure 3, the electron density during daytime increases monotonically with altitude right up to the rocket apogee. On some of the flights a decrease in electron density of about 10% is observed around 115 km altitude. On all the flights large upward gradients were observed below 100 km altitude. During nighttime, due to the jagged nature of the density profile, regions of both upward and downward gradients are present over a much wider range of altitude compared to the daytime. Table 1 gives the region of occurrence of M_c irregularities observed during different times of the day (Sinha 1976).

It can be seen from table 1 that during daytime the irregularities can be seen continuously in the altitude range of 87·5 to 100 km, whereas during evening and nighttime they are observed in many isolated regions. Further, while during daytime and evening they are seen only in the regions of positive density gradients, during nighttime they are seen only in regions of negative density gradients. It must be noted here that during daytime and evening time the Hall polarization field is vertically upward whereas during the nighttime it is downward. Thus M_c irregularities are seen only where the electron density gradients and the Hall polarization fields are in the same direction. Further, during the two counter electrojet periods (figure 6) when the

Table 1. Type M_c irregularities.

Period of observation and flight No.	Altitude region of occurrence
Daytime flight No. 10.44 on Oct. 13, 1972 at 1259 hr (IST)	Observed continuously from 88·5 to 96·6 km, in the region of upward density gradient.
Daytime flight No. 10.45 on March 3, 1973 at 1259 hr (IST)	Observed continuously from 87·5 to 110 km in the region of upward density gradient.
Evening time flight No. 10.13 on Feb. 2, 1968 at 1856 hr (IST)	Observed from 86·5 to 88 km, 89·8 to 90·7 km, 92·2 to 93·2 km, 96·5 to 98·0 km in the regions of upward density gradients.
Nighttime flight No. 20.08 on August 29, 1968 at 2300 hr (IST)	Observed from 94 to 96·5 km, 97·5 to 98·8 km, 109·2 to 110·5 km, 117·4 to 118·4 km, 119·2 to 120·2 km, 121·2 to 121·9 km in the regions of downward density gradient.
Nighttime flight No. C-21 on April 21, 1975 at 2300 hr (IST)	Observed from 102 to 103·2 km, 105·7 to 107·7 km, 111·3 to 115 km in the regions of downward gradient.
Daytime flight No. CO-5.16 on Aug. 17, 1972 at 15·32 hr (IST)	Observed in the 97 km region in the region of downward density gradient.

Hall polarization field is believed to be downward, M_c irregularities were seen only in the regions of downward density gradients (Prakash *et al* 1979a). Hence these results are in excellent agreement with the theory of cross field instability mechanism which requires the electron density gradients to be in the direction of the electric fields for its growth. Klaus and Smith (1978) presented the results on M_c irregularities obtained from one daytime and two nighttime rocket flights from Chilca, Peru. While the results for the daytime and one of the nighttime flights agree with earlier results from Thumba, the results from the other nighttime flights differ and no preferred direction of the electron density gradients was seen in the region of occurrence of M_c irregularities. It may be pointed out that M_c irregularities were observed on all the flights from Thumba except the one which was carried out during the period when the electrojet fields was very weak. The scattered signals from M_c irregularities can sometimes be clearly seen with an ionosonde (Rastogi 1972).

3.1b *Shape of the irregularities*: A visual inspection of telemetry data on M_c irregularities reveals the characteristic shape of these irregularities. Figure 7 gives the telemetry record for two noontime flights corresponding to different altitudes (Sinha 1976). The total length of the data corresponds to about 1·4 km. The arrow denotes the direction in which the density increases. It can be seen from figure 7 that in the direction of increasing density, the structures exhibit sharper rise than fall thereby giving them

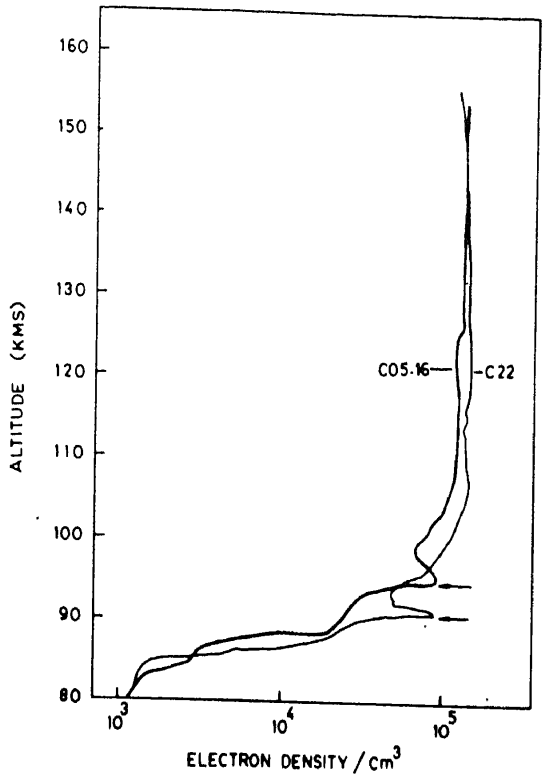

Figure 6. Electron density profile during the daytime in the counter electrojet periods. The density profiles obtained during the rocket ascent of flights CO 5·16 and C-22 are plotted. The arrows indicate the location of the ionization layers seen on these flights.

the sawtooth shape. The sawtooth character of the structures is evident at 90 km for the 10·44 flight and at 87·5 km for the 10·45 flight. At higher altitudes the sawtooth shapes are somewhat distorted. It may be pointed out that the sawtooth structures are seen more clearly during daytime. Rognlien and Weinstock (1974) used a two-dimensional code to study the saturated amplitude and to explain the sawtooth structures for the nighttime conditions. The theory could not explain these structures during daytime.

3.1c *Amplitude of the irregularities*: The percentage amplitude of M_c irregularities can be as large as 30%, both during daytime and nighttime. During daytime normal electrojet the percentage amplitude of the M_c is maximum around 90 km. Due to high variability of the evening and the nighttime electron density profiles, the region of maximum irregularity amplitude varies from flight to flight, for example, on flight 20·08 they were observed in the 90 to 120 km region.

3.1d *Spectral index*: The power spectrum of M_c irregularities was determined assuming a power law of the form $P(k) \propto k^n$ where $P(k)$ is the spectral density at the scale size corresponding to the wavenumber k, and n is the spectral index. The power spectrum of M_c irregularities observed on the flight 10·45 at three different altitudes is shown in figure 8. The spectrum is steeper at 87·5 km than at higher altitude. This

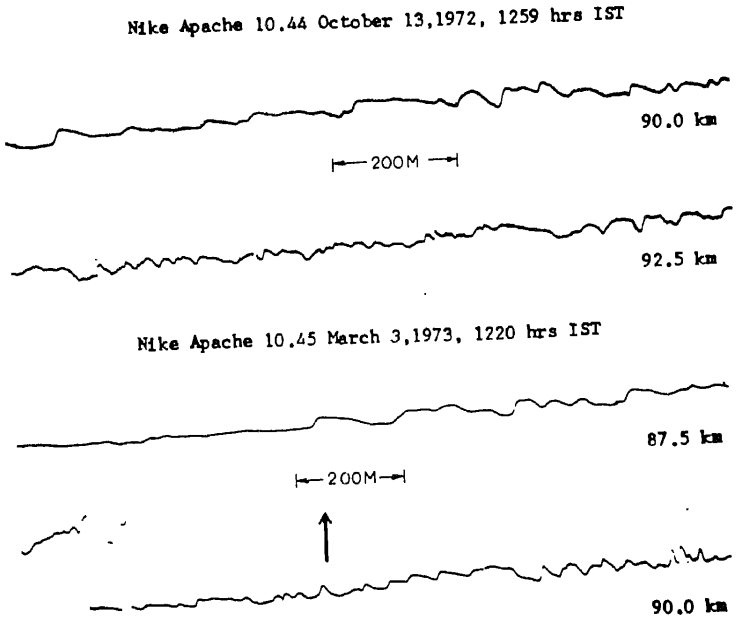

Figure 7. Typical sawtooth shapes of the type M_c irregularities observed on the flights 10·44 and 10·45 at two different altitudes. The data shown is the real time T/M output corresponding to about 1·4 km altitude range. The vertical arrow denotes the direction in which the density is increasing.

feature was obtained for almost all the daytime flights. The spectral index obtained for M_c irregularities from three rocket flights was in the range $-2 \pm 0{\cdot}7$ (Sinha 1976). It may be noted here that this range of the spectral index was calculated from M_c irregularities data obtained in the altitude range of 87 to 92 km. Using a two-dimensional code, Rognlien and Weinstock (1974, 1975) found n to be $\simeq -2$.

3.2 *Small scale irregularities (type S_c)*

The small scale type S_c irregularities in the scale size range of 1–15 m have been observed on all the flights carried out during different times of the day (except the one mentioned earlier). They coexist with M_c irregularities (Prakash *et al* 1969; 1970; 1972a; Sinha 1976). Hence their region of occurrence is the same as has been summarised in table 1 for M_c irregularities. Their amplitude was small in comparison to M_c, and was a few percent. The left half of figure 9 gives a typical record of S_c irregularities around 93·5 km and the right half gives that of S_s irregularities around 105 km. The bottom-most channel in figure 9 gives the composite amplitude of these irregularities in 1–15 m scale size range. Starting from the topmost channel, the six channels give the amplitude of the irregularities in different scale size ranges. From the left half of the figure it can be seen that S_c irregularities appear in the form of bursts whose separation could be anywhere between a few tens-of-meters to hundreds-of-meters. During daytime the bursts of the irregularities were seen in the altitude range of 87 to 96 km. Up to 91 km, their location matched very well with the rising parts of the sawtooth structures observed for M_c

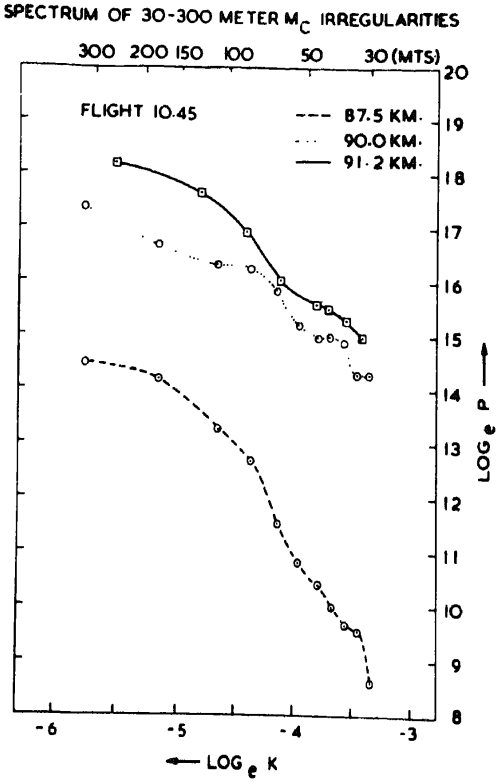

Figure 8. Power spectrum of type M_c irregularities calculated at three different altitudes for the flight 10·45. It is evident that the power is maximum around 90–91 km altitude.

irregularities. Above 96 km, however, small scale irregularities were observed more or less continuously, though with varying amplitudes eventually merging with S_s irregularities (to be discussed later). No clear distinction can be made between S_c and S_s near the peak of the electrojet from *in situ* measurements. During nighttime, M_c irregularities were observed right up to 120 km and S_c irregularities were observed wherever M_c were observed.

The coexistence of M_c and S_c irregularities indicates that the latter are produced through the former *via* some secondary processes. The spectral index of S_c irregularities was highly variable with altitude. The spectral index for one of the daytime flights given in table 2 (Sinha 1976) shows that the steepness of the spectrum decreases with altitude. McDonald *et al* (1975) studied nonlinear evolution of small scale irregularities. The spectral index from their theory was $-3{\cdot}5$. The laboratory experiment by Saxena and John (1975) gave a spectral index of $-3{\cdot}8$. As pointed out earlier, in the 105 km altitude region, S_c irregularities merge with S_s, hence only those below this altitude can be purely due to the cross field plasma instability mechanism.

4. Irregularities produced through the streaming of electrons (type S_s)

Type S_s irregularities (1–15 m) were observed during daytime in the 105 km region when the electrojet currents were strong (Prakash *et al* 1971). The amplitude of these

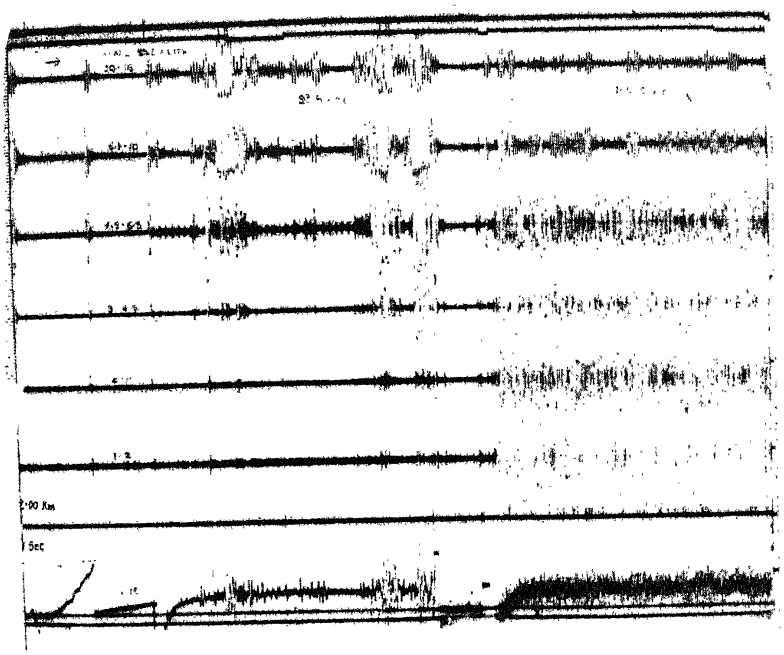

Figure 9. Typical T/M record showing the small scale irregularities at 93·5 and 105·5 km altitude. The left half of the figure corresponds to the type S_c irregularities which are seen in well-separated regions in the form of bursts. The right half of the figure shows type S_s irregularities occurring more or less continuously. The lowest channel gives the composite amplitude of the irregularities in 1–15 m scale size range. The other channels give the spectral output in different scale size bands noted on each channel. Starting from the top the outputs correspond to scale sizes 15-10, 10-6·5, 6·5-4·5, 4·5-3, 3-2 and 2-1·3 m respectively.

Table 2. Spectral index of the type S_c irregularities at different altitudes (flight 10.45).

Altitude (km)	Spectral index n
90·8	−5·1
92·3	−4·9
94·2	−5·0
96·6	−3·8
97·7	−3·7

irregularities which is normally a few percent of the background density has been observed to peak at around 105 km altitude. A typical telemetry chart showing their presence is given in the right half of figure 9. The percentage amplitude of S_s irregularities in relation to the density, electric current and electron drift velocity is given in figure 10. The amplitude of 1–15 m irregularities below 96 km was not plotted in this figure as their amplitudes were highly variable.

It can be seen from the figure that S_s irregularities are better correlated with the streaming velocity of the electrons than with the gradients in the electron density. Also their amplitude is seen to be quite appreciable above 110 km. VHF radar studies (Fejer *et*

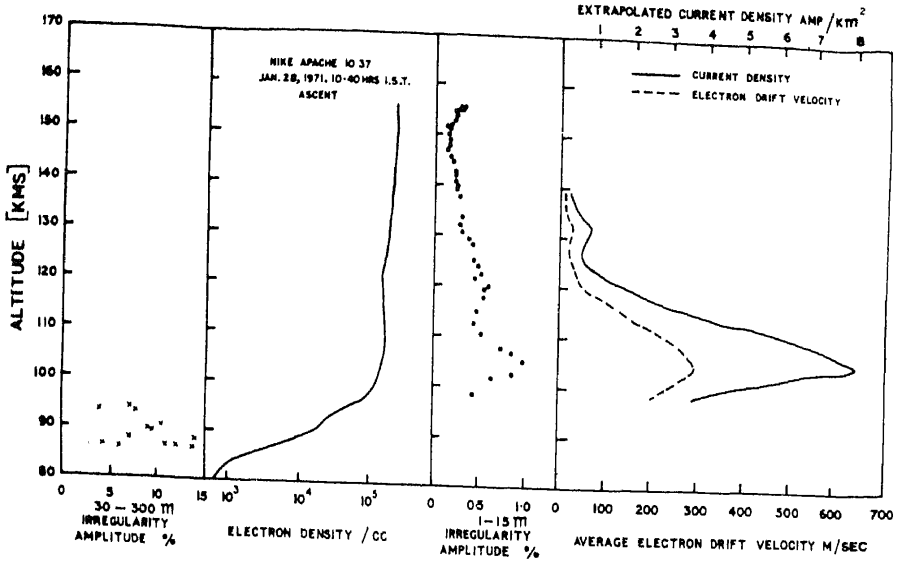

Figure 10. Profiles of the electron density, current density, relative electron-ion drift velocity and percentage amplitude of 30–300 m and 1–15 m scale size irregularities observed on the daytime flight 10·37 from Thumba. Amplitude of 1–15 m irregularities below 100 km was not plotted as it was highly variable. Note that the relative electron-ion drift velocity is less than 300 m/sec even at the peak of the electrojet.

al 1975) during daytime do not show the presence of irregularities above 113 km altitude in contrast to the rocket results. Recent measurements at Chilca (Klaus and Smith 1978) agree with the rocket results from Thumba. It may, however, be pointed out that on many flights small scale (1–15 m) irregularities were not observed above 110 km altitude. It can therefore be concluded that the conditions required to generate irregularities above 110 km are satisfied only on some of the days. There is probably another mechanism operating above 110 km. The spectral index of irregularities in the range 1–10 m around 105 km was nearly zero on all the flights. On flight C05-16 during counter electrojet period, the scale size of these irregularities was less than 7 m while during normal electrojet it extended right up to 15 m. During a strong counter electrojet event Crochet *et al* (1979) found the nature of type I spectra to be different than during normal electrojet events.

5. Electron density irregularities and electric fields

The electrostatic plasma instability mechanisms which are responsible for the generation of electron density irregularities in this region are driven by the free energy available in the medium. During the process of formation of irregularities the initial perturbation in electron density gives rise to localised polarization electric fields due to charge separation. These fields give rise to plasma transport in such a way that the amplitude of perturbation grows in time which in turn gives rise to increasing polarization fields. The perturbation in electron density and these polarization fields

continue growing till the growth rate becomes comparable with the decay rate. The polarization fields are therefore an inseparable part of the plasma instability mechanisms prevalent in this region. For a clear understanding of a plasma instability mechanism, it is necessary to understand the nature of these fields which give a macroscopic picture of the plasma transport. It has now been possible to measure simultaneously the electron density irregularities and electric fields in both the horizontal and vertical direction (Pal *et al* 1983). Thus the study of two-dimensional transport of plasma due to various plasma instability mechanisms operating in the E and F region has now become possible.

Simultaneous measurement of structures in the electron density and electric field has been recently carried out from Thumba, India during daytime (Prakash *et al* 1983) when the electrojet currents were strong enough to give type I radar echoes. The sensors A and B in figure 2 are used to measure electric field along the spin axis of the rocket and sensors C and D for the electric field perpendicular to the spin axis of the rocket. These can also be considered as representatives of the vertical and horizontal electric fields respectively.

During flight C-77 the Langmuir probe was operated in the sweep mode with bias varying from +4 V to zero. The probe was switched on and off alternately and this cycle was repeated throughout the flight. Although the sweep voltage mode of operation is not suited for a detailed study of the electron density irregularities, their shape and regions of occurrence could be very well ascertained.

In the frame of reference of the rocket, the electric field E is given by $E = E' + V \times B$ where E' is the ambient field and $V \times B$ is the induced field due to the motion of the rocket. As $(V \times B)$ changes slowly with time, the faster variation in E' can be studied with E without correcting it for the $V \times B$ field. Figure 11 gives the vertical electric field (E_V) at different altitudes as observed on C-77 flight on 12 February 1981 at 10·57 hr (IST) from Thumba (Prakash *et al* 1983). It can be seen that the structures in electric field were of largest amplitude in the altitude range of 90 to 100 km which is also the region of upward gradients in electron density and where type M_c and S_c irregularities were observed. These structures had scale sizes ranging from few meters to few km. The largest amplitude was observed for scale sizes of less than a few hundred metres, some of them having peak-to-peak amplitude up to 20 mV/m. Type S_s irregularities were observed in 104 km region and irregularities in E_V and E_H associated with it were clearly seen. Above 106 km the sinusoidal variation in the electric field is due to the spin of the rocket. The triangular shape in 88 km region are due to the interaction of sensor B with the side booms supporting sensors C and D.

The spin of the rocket gives a spin modulation to the horizontal electric field measurement. This spin dependence was eliminated by dividing the data by appropriate unit sine wave. Figure 12 gives the amplitude of field E_H in one of the flights. A number of structures with peak to peak amplitudes as large as 16 mV/m and vertical scale sizes up to 10 km in the altitude range of about 90 to 105 km can be seen in the figure. The mechanism of production of these large scale fields is not yet clear. One of the promising mechanisms is the crossfield instability mechanism.

A gradual decrease in the value of electric field E_H with altitude is due to decrease in the vertical velocity of the rocket. The structures seen above 130 km altitude are due to the rocket precessions which are not discernible at lower altitudes. In the lower altitude regions the structures due to the rocket precession have not only large separation but also they are masked by the prevalent structures in the horizontal field. As has been

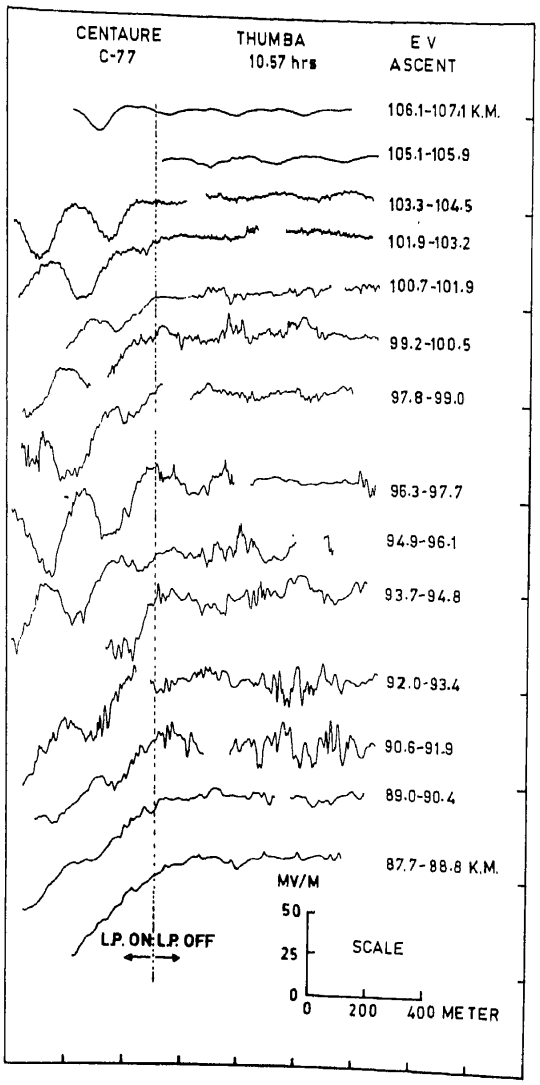

Figure 11. Telemetry record showing fluctuations in vertical electric field at different altitudes on a daytime flight C-77. The total length of the record corresponds to about 1·2 km altitude range. The left part of the data which is divided by drawing a dashed vertical line corresponds to the period when the onboard Langmuir probe was on and hence is contaminated. The portion on the right of the vertical line is free from this contamination.

noted earlier, the largest fluctuations in the electric fields were observed in the 90 to 105 km altitude region, which covers the region where M_c and S_c irregularities are usually observed. Visual inspection of the telemetry channels shows that the fluctuations in electron density, vertical and the horizontal electric field with scale sizes less than a few hundred meters show a definite correlation between themselves.

Pfaff *et al* (1982) have reported the results of two rocket launches for measuring horizontal electric fields with the double probes, one during the daytime from Chilca (mag. dip = 0·5°) when the electrojet currents were strong and the other from the island

Table 3. Summary of the ionization irregularities in the equatorial *D* and *E* region based on rocket and ground based experiments.

Generation mechanism	Type of irregularity	Scale size and shape	Region and time of observations	Max. peak to peak amp.	Range of spectral index	Backscatter radar observations	Ionosonde observations and additional remarks
Crossfield instability	M_c	(30–300)m Many of them of sawtooth shape	Between 85–140 km wherever E‖V Ne. Most of the times.	30%	$-2 \pm 0{\cdot}7$	—	Esq. at lower frequencies
	S_c	(1–15)m	-do-	2%	$-3{\cdot}5 \pm 1{\cdot}5$	Responsible for type II echoes	Used for the determination of the phase velocity of the irregularities.
Streaming instability	S_s	(1–15)m	Around 105 km where V_d is large. Mostly around noon	2%	0	Responsible for type I echoes	Esq. present at higher frequencies Dominates over Sc in 106 km region
Neutral turbulence induced	M_n	(30–300)m	Below 80 km	20%	$-2{\cdot}7 \pm 0{\cdot}4$	—	—
	S_n	(1–15)m	Below 80 km	2%	$-1{\cdot}6 \pm 0{\cdot}7$	Observed with powerful radars	Used for the study of the mesospheric winds
Gravity wave winds	L	Horizontal tens-of-km Vertical few km	In 80–130 km during night. In 90–95 km during daytime CEJ	Varies by a factor of 25	—	—	Many layers during night. Only one layer during day time CEJ*. No layers during NEJ*.
Rocket induced	S_R	Few meters	Near apogee in the night and evenings	—	+ ve	—	The spectral index is + ve as only lower end of the spectrum is seen

* CEJ – Counter electrojet; * NEJ – Normal electrojet.

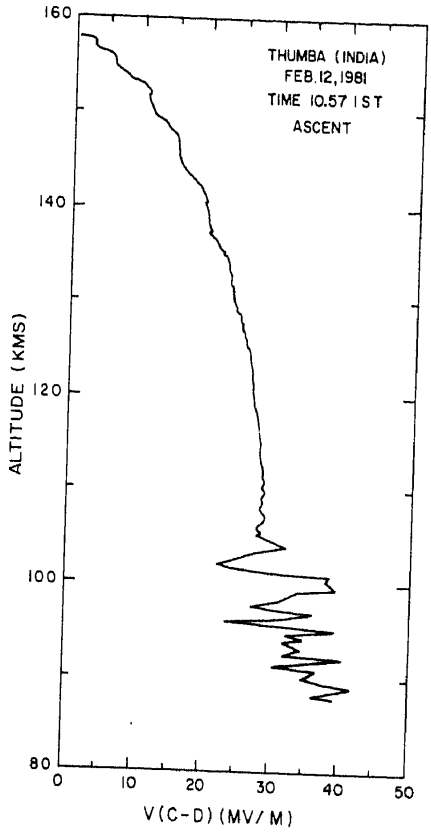

Figure 12. Altitude variation of the horizontal electric field measured on the daytime flight C-77. The $V \times B$ field has not been subtracted from these measurements.

of Kwajalein (mag. dip = 9°) during nighttime. From their experiments the electric field fluctuations were observed mostly in the region where the condition for the excitation of crossfield plasma instability was satisfied. These results were similar to those observed at Thumba.

6. Irregularities due to the neutral turbulence

VHF radar studies by Woodman and Guillen (1974) revealed electron density irregularities at the mesospheric heights (55 to 85 km). The motion of these irregularities is used to study the dynamics of this region. Since the *D* region plasma is highly collisional, and the neutral turbulence is the only well-established process which can give rise to electron density irregularities in this region, the mesospheric electron density irregularities have been attributed to the neutral turbulence. The irregularities were classified into M_n and S_n according to their scale sizes.

The Thumba measurements revealed the presence of M_n and S_n irregularities in the altitude range of about 70 to 80 km (Sinha 1976). Their amplitude distribution was highly variable with altitude, and from flight to flight.

6.1 *Type M_n irregularities*

Figure 13 shows the telemetry record for the flight 10·45 corresponding to an altitude of 77·5 km. The total length of the record corresponds to about 1·8 km altitude range. The channels 1, 2 and 3 correspond to the DC current to the Langmuir probe, fluctuations in the probe current in the 30–300 m scale size range and in the (1–15 m) scale size range respectively. An inspection of channel 2 reveals that the medium scale fluctuations do not have any characteristic shape. The amplitude of irregularities in this region was $\approx 5\%$.

Figure 14 shows the power spectrum of M_n irregularities observed during flight

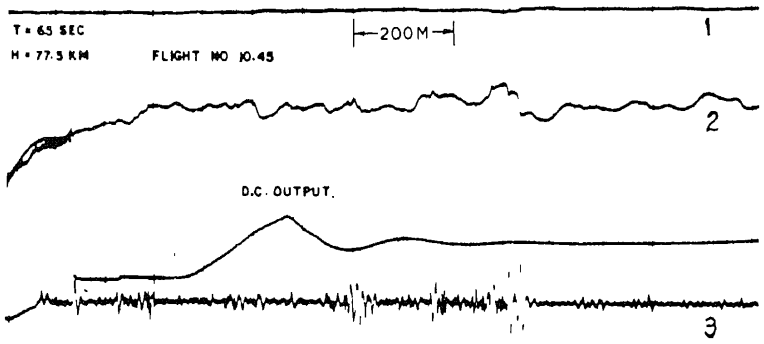

Figure 13. *T/M* record showing the electron density irregularities produced due to the neutral turbulence. The data was obtained on a daytime flight 10·45 from Thumba. The length of the record corresponds to about 1·8 km altitude range. The channels marked 2 and 3 show the presence of the type M_n and type S_n irregularities respectively.

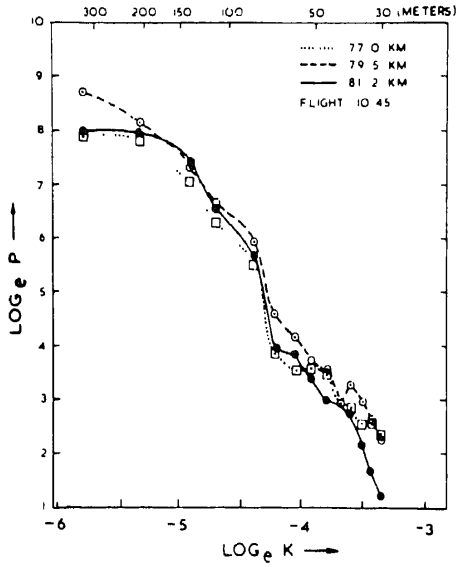

Figure 14. Power spectrum of the type M_n irregularities calculated for the daytime flight 10·45 at three different altitudes.

10·45, at three altitudes, *viz* 77, 79·5 and 81·2 km. The average spectral index in this range of altitude is about −2·9. The spectral index at 70·5 km altitude for another flight was −2·3 (Sinha 1976). On the average, the spectral index for M_n can be represented by $-2{\cdot}7 \pm 0{\cdot}3$.

6.2 *Type S_n irregularities*

The S_n irregularities were observed more frequently than M_n due to large gain in the system corresponding to 1–15 m scale size range. As noted earlier, these irregularities were observed along with M_n in 60 to 80 km altitude range. Type S_n irregularities were seen more prominently below 70 km altitude. Channel 3 of figure 13 shows a typical record of these irregularities. The power spectrum of S_n irregularities was highly variable with height and from flight to flight. For example, on one of the flights, C0-5·14 at 0745 hr IST, the spectral index at 61·9, 63·9, 66·2 and 68·2 km altitude was respectively −1·4, −1·1, −1 and −0·9. For another flight 10·37 the spectral index was respectively, −2·1, −2·1, −2·2 at altitude of 61·4, 63 and 70·3 km. For all flights, the range of the spectral index was $-1{\cdot}6 \pm 0{\cdot}7$.

7. Responsible for the type I and type II spectra irregularities

As pointed out earlier, electron density irregularities could not be studied in detail with ground-based VHF radar and rocket-borne experiments. While the radar gives the temporal and spatial variation of the irregularities and their drift velocity, the rocket experiments give the high resolution data and the other localised parameters relevant for these studies. A summary of the ionization irregularities in the equatorial D and G regions is given in table 3.

A comparison of characteristic features of the small scale irregularities, for example the spectral index, time and region of occurrence, observed with the rocket experiments and those with the VHF radar indicates that type II spectra are due to S_c irregularities, and the type I due to S_s irregularities (Prakash *et al* 1973). Following are some of the salient features. Figure 15 shows the RTI diagram of the VHF radar at Jicamarca at different times of the day (Fejer *et al* 1975). It can be seen that during daytime the radar echoes come from a continuous region extending from 93 to 113 km. During nighttime, however, the echoes come from a much wider altitude range. Distinct gaps are seen in the RTI diagrams from where no scattering takes place. These results are in excellent agreement with rocket observations as far as the region of occurrence of the irregularities is concerned. Rocket results also show the presence of S_c irregularities from about 87 to 96 km where the gradients in the density are strong during daytime. As the region of peak electrojet currents is reached (where the gradients in density are insignificant), S_s irregularities take over S_c. During nighttime, rocket results show very well-separated regions where M_c and S_c irregularities are seen. This strongly indicates that type II echoes come from regions where M_c and S_c irregularities are observed.

VHF radar observations at 16, 50 and 146 MHz corresponding respectively to the irregularity scale sizes 9, 3 and 1 m, indicate that the power *vs* wavenumber spectra for the type II irregularities are steeper than for type I irregularities (Balsley and Farley

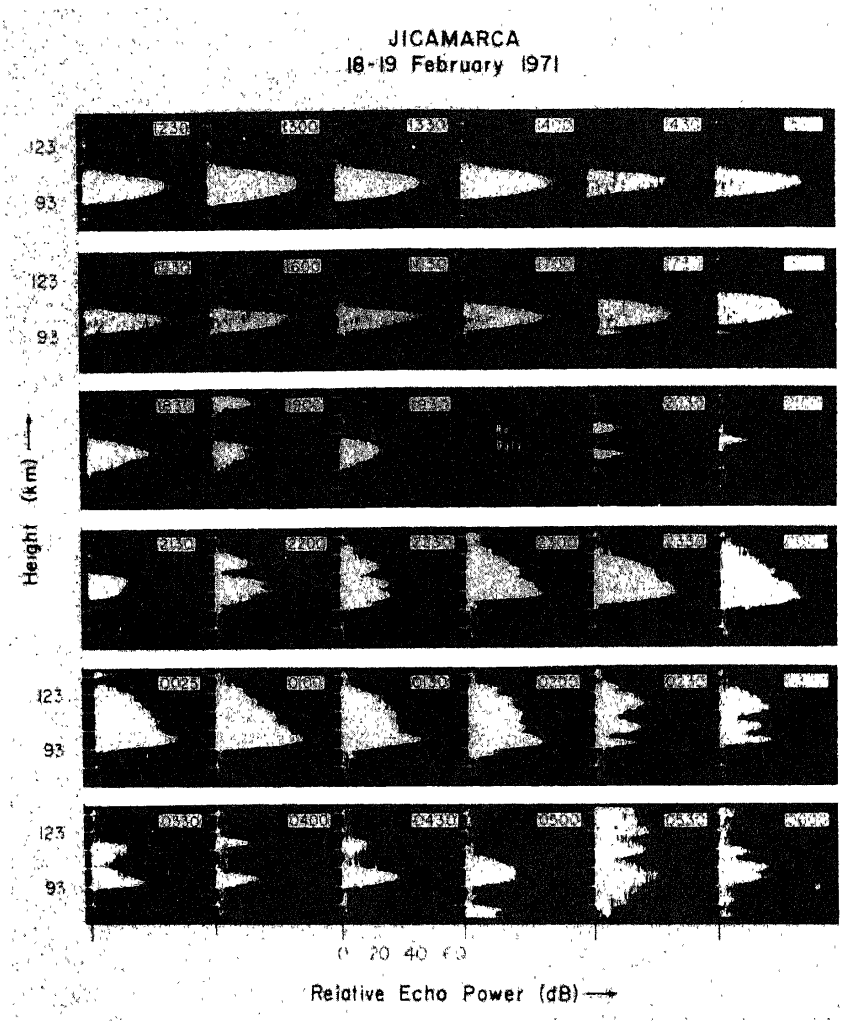

Figure 15. Intensity of the back scattered radar signal from the *E* region irregularities during different times of the day (From Fejer *et al* 1975).

1971). As shown earlier, rocket results also reveal that power spectra for S_c irregularities are much steeper than for type S_s.

8. Outstanding problems

The mechanisms which can give rise to electron density irregularities in the *E* region are (i) the crossfield ($E \times B$) instability, (ii) the two-stream instability and (iii) the large scale plasma transport by winds and electric field. Various theories of the first two mechanisms have been well reviewed (Fejer and Kelley 1980). Following are some of the outstanding problems which are not yet well understood.

8.1 *Type S_s irregularities*

A linear theory of two-stream instability mechanism applicable to the ionospheric E region was developed by Farley (1963) and Bunneman (1963) to explain type I irregularities which shows the plasma to be unstable when the relative electron-ion drift velocity exceeds the ion acoustic velocity in the medium. Farley (1963) showed that maximum linear growth occurs for waves having a wavelength of about 3 m. Since the ion acoustic velocity at the E region altitudes is about 360 m/sec, a threshold drift velocity requirement is explicit to excite the two-stream instability. Later modification by Sudan *et al* (1973) have made the threshold requirement all the more stringent $V_d > C_s(1+\psi)$ where V_d is the relative electron-ion drift velocity, C_s is the ion acoustic velocity in the medium, $\psi = \nu_e \nu_i / \Omega_e \Omega_i$, $\nu_{i,e}$ being the ion, electron-neutral collision frequencies and Ω_e, Ω_i being the electron and ion gyrofrequencies respectively. Recently Sudan (1983) proposed a nonlinear theory for the two-stream instability mechanism based on the kinetic theory of the plasma which makes an attempt to explain some of the features of the type I irregularities.

For a given value of the east-west electric field and assuming a simple model of the electrojet, $V_d/(1+\psi)$ will be maximum where $\psi = 1/3$ (Fejer *et al* 1975). Thus, to satisfy the threshold requirement, V_d should be larger than 480 m/sec. Rocket experiments were conducted at Thumba with combinations of Langmuir probe, mutual admittance probe and proton precession magnetometer at times when the ground-based VHF radar showed type I irregularities. The studies revealed that type I irregularities were present although the drift velocity was less than 360 m/sec. This value is already much less than the threshold value for the excitation of the two-stream instability. This shows that either the present development of the plasma instability theories is incomplete or that strong localised currents are present (besides the electrojet currents) in order to satisfy the threshold requirement in the localised region. The presence of localised current has been indicated from various studies; however a quantitative picture is not yet clear. Recent electric field measurements show the presence of large fluctuating fields in the 90–105 km region (Prakash *et al* 1983). Studies with VHF radar in the equatorial electrojet region (Reddy and Devasia 1976) indicated the existence of fluctuating currents with periods similar to those of the gravity waves. Theoretical studies by Prakash and Pandey (1979) show that substantially large fluctuating currents can be generated by gravity wave winds to meet the threshold requirements at least partially. Another feature of type I irregularities is the phase velocity of irregularities which is independent of the electron-ion drift velocity and the elevation angle of the radar. Presently available theories (Kaw 1972; Lee and Kennel 1973; Farley and Balsley 1973) which use the convective nature of these irregularities, have not been able to explain these observations satisfactorily.

8.2 *Type S_c irregularities*

While the theories of crossfield instability can to a certain extent explain the generation and shape of M_c irregularities, the theories for type S_c irregularities have not come to a satisfactory stage. Sudan *et al* (1973) had developed a two-step theory to explain small scale irregularities. The theory predicted a minimum wavelength given by

$$\lambda_{\min} = 8 A^{-1} V_d^{-3/4} \text{ m}$$

For an electron drift velocity of 100 m/sec and peak-to-peak amplitude $A = 4\%$ the $\lambda_{min} = 6$ m. Rocket-borne studies have shown that irregularities with scale sizes down to at least 1 m are present in the region where A is even less than 4%. Recently electric fields with peak-to-peak amplitudes up to 16 mV/m have been observed in 90 to 105 km region (Prakash *et al* 1983). These may have to be incorporated in the theories to explain the observed results.

8.3 *Large scale electric fields in the E region*

Electric field with vertical scale sizes as large as 6 km and peak-to-peak, amplitudes as large as 16 mV/m have been observed (Prakash *et al* 1983). The theories to explain many of the features of these fields are yet to be developed.

8.4 *Large scale irregularities (type L)*

Large scale irregularities observed during daytime counter electrojet require a large columnar density of ions which have lifetime of at least a few hours. Such ions have not yet been identified.

8.5 *Effect on equatorial electrojet*

Rocket-borne studies (Subbaraya *et al* 1972) show that the electrojet currents peak at an altitude of 3 km higher than that expected from model calculations using collision frequencies as derived from standard neutral density models. To account for these discrepancies an increase of collision frequency by a factor of three, both for ions and electrons, is required. Whether the observed plasma density irregularities and the electric field irregularities can modify the collision frequencies by such a large factor should be explored.

In this paper only very major anomalies between observations and the present theoretical development are listed. There are a large number of detailed features of the experimental observation for which suitable theories have to be developed.

Acknowledgements

The authors are thankful to all the scientific and technical personnel involved in the scientific work reviewed here. Due to their involvement with the rocket experiments from Thumba, the authors feel highly obliged to all the staff members of the Thumba Equatorial Rocket Launching Station (TERLS), Space Physics Division (SPD) and Physical Research Laboratory (PRL) who contributed to the success of the experiments. Special mention is made of Prof. V A Sarabhai who initiated the programme at Thumba and the active co-operation of Messrs A P J Abdul Kalam, R Arvamudam, V Sudhakar, Madhavan Nair and A C Bahl of TERLS, Dr C A Reddy of SPD, Prof T S G Sastry, Prof B H Subbaraya, Dr S P Gupta, Dr H S S Sinha, Mr S Pal, Mr R N Misra and Mr Y B Acharya of PRL.

References

Anandarao B G, Raghavarao R and Reddy C R 1977 *J. Geophys. Res.* **82** 1510
Axford W I 1963 *J. Geophys. Res.* **68** 769
Balsley B B 1967 *Tech. Memo.*, IERTIM-ITSA 89
Balsley B B 1969 *J. Geophys. Res.* **74** 2333
Balsley B B and Farley D T 1971 *J. Geophys. Res.* **76** 8341
Bowles K L, Balsley B B and Cohen R 1963 *J. Geophys. Res.* **68** 2485
Bowles K L and Cohen R 1962 in Ionospheric Sporadic E (eds) E K Smith and S Matsushita (London: Pergamon Press)
Bowles K L, Cohen R, Ochs G R and Balsley B B 1960 *J. Geophys. Res.* **65** 1853
Bunneman O 1963 *Phys. Rev. Lett.* **10** 285
Cohen R and Bowles K L 1967 *J. Geophys. Res.* **72** 2222
Crochet M, Hanuise C, Broche P 1979 *J. Geophys. Res.* **84** 5223
Egan R D 1960 *J. Geophys. Res.* **68** 2343
Farley D T 1963 *J. Geophys. Res.* **68** 6083
Farley D T, Balsley B B 1973 *J. Geophys. Res.* **78** 227
Fejer B G, Farley D T, Balsley B B and Woodman R F 1975 *J. Geophys. Res.* **80** 1313
Fejer B G and Kelley M C 1980 *Rev. Geophys. Space Phys.* **18** 401
Hoh F C 1963 *Phys. Fluids* **6** 1184
Kato S 1973 *J. Geophys. Res.* **78** 757
Kaw P K 1972 *J. Geophys. Res.* **77** 1323
Keskinen M J 1981 *Phys. Rev. Lett.* **47** 344
Klaus D E and Smith L G 1978 Aeronomy Rep. No. 80, Uni. of Illinois, Urbana, USA
Knox F B 1964 *J. Atmos. Terr. Phys.* **26** 239
Lee K and Kennel C F 1973 *Planet. Space Sci.* **121** 1339
Lee K, Kennel C F and Coroniti F V 1974 *J. Geophys. Res.* **79** 249
Maeda K, Tsuda T and Maeda H 1963 *Phys. Rev. Lett.* **11** 406
Matsushita S 1951 *J. Geomag. Geoelec.* **3** 44
Mc Donald B E, Coffey T P, Ossakow S L and Sudan R N 1975 *Radio Sci.* **10** 247
Morse D L 1965 *Phys. Fluids* **8** 1339
Pal S, Prakash S, Acharya Y B and Misra R N 1983 *Adv. Space. Res.* 7 57
Pandey R 1981 Ph.D. Thesis submitted to Gujarat Uni. India
Pfaff R F, Kelley M C, Fejer B G, Maynard N C and Baker K D 1982 *Geophys. Res. Lett.* **9** 688
Prakash S, Gupta S P and Subbaraya B H 1969 *Radio Sci.* **4** 791
Prakash S, Gupta S P and Subbaraya B H 1970 *Planet. Space Sci.* **18** 1307
Prakash S, Gupta S P and Subbaraya B H 1971 *Nature (London)* **230** 170
Prakash S, Gupta S P, Subbaraya B H and Pandey R 1979a *Space Res.* **19** 279
Prakash S, Gupta S P, Subbaraya B H and Pandey R 1979b Low Lat. Aeronomical Processes, COSPAR Sympos. Series **8** 3
Prakash S, Gupta S P, Subbaraya B H, Sinha H S S and Jain C L 1973 Paper presented at I Lloyd V. Berkner Sympos. AGU, Univ. of Texas USA
Prakash S and Subbaraya B H 1967 *Rev. Sci. Inst.* **38** 1132
Prakash S, Subbaraya B H and Gupta S P 1972a *Indian J. Radio Space Phys.* **1** 72
Prakash S, Subbaraya B H and Gupta S P 1972b Aeronomy Report No. 48 Univ. of Urbana
Prakash S, Jain C L, Balsley B B and Greenwald R A 1974 *J. Geophys. Res.* **79** 334
Prakash S, Pal S and Pandey R 1983 *Adv. Space Res.* **2** 93
Prakash S and Pandey R 1979 *Proc. Indian Acad. Sci.* **A88** 229
Rao T R and Prakash S 1978 *Space Res.* **18** 281
Rastogi R G 1972 *Nature (London)* **237** 73
Rastogi R G 1974 *J. Geophys. Res.* **79** 1503
Reddy C A and Devasia C V 1976 *Nature (London)* **261** 39
Reid G C 1968 *J. Geophys. Res.* **73** 1627
Rogister A 1971 *J. Geophys. Res.* **76** 7745
Rogister A and D'Angelo N 1970 *J. Geophys. Res.* **75** 3819
Rognlien T D and Weinstock J 1973 *J. Geophys. Res.* **76** 6808
Rognlien T D and Weinstock J 1974 *J. Geophys. Res.* **79** 4733

Sampath S 1976 Ph.D. Thesis submitted to Gujarat Univ. India
Sartiel J 1977 Ph.D. Thesis, University of Paris
Sato J 1972 *Phys. Rev. Lett.* **28** 732
Saxena Y C and John P I 1975 *Geophys. Res. Lett.* **2** 492
Simon A 1963 *Phys. Fluids* **6** 382
Singer S F, Mapel E and Bowen W A 1951 *J. Geophys. Res* **56** 265
Sinha H S S 1976 Ph.D. Thesis submitted to Gujarat University, India
Smith L G and Mechtly E A 1972 *Radio Sci.* **7** 367
Subbaraya B H, Muralikrishna P, Sastry T S G and Prakash S 1972 *Planet. Space Sci.* **20** 47
Sudan R N 1983 *Geophys. Res. Lett.* **10** 983
Sudan R N, Akinrimisi J and Farley D T 1973 *J. Geophys. Res.* **78** 240
Weinstock J and Sleeper A 1972 *J. Geophys. Res.* **77** 3621
Whitehead J 1961 *J. Atmos. Terr Phys.* **20** 49
Woodman R F and Guillen A 1974 *J. Atmos. Sci.* **31** 493